Successive structural phase transitions in monoclinic thallium monosulphide

1993 J. Phys.: Condens. Matter 5 4243

(http://iopscience.iop.org/0953-8984/5/25/014)

J. Phys.: Condens. Matter 5 (1993) 4243–4250. Printed in the UK

Successive structural phase transitions in monoclinic thallium monosulphide

S Kashida†, K Nakamura† and S Katayama‡

† Department of Physics, Niigata University, Ikarashi, Niigata, 950-21, Japan
‡ College of General Education, Niigata University, Ikarashi, Niigata, 950-21, Japan

Received 23 November 1992, in final form 8 February 1993

Abstract. The structural phase transitions in newly found monoclinic TlS have been studied using single-crystal x-ray diffraction methods. The room temperature ferroelectric phase has a commensurate structure; the satellite reflections are observed at $q_c = (0, 0, \frac{1}{4})$ suggesting fourfold lattice modulations along the c axis. The intermediate phase between 318.6 K and 341.1 K is incommensurate; the satellites shift from q_c to $q_i = (0.04, 0, \frac{1}{4})$. In the high-temperature paraelectric phase above 341.1 K, these satellite reflections disappear. A phenomenological treatment of the successive phase transitions in TlS is given. The temperature dependence of the dielectric constant is also discussed. The experimental results are compared with those for $TlGaSe_2$.

1. Introduction

Binary compounds in the thallium–sulphur system have been known for a long time, and have attracted practical interest as photo-detectors (see, for example, Asai [1] and a recent article by Nagat [2]). However, the fundamental properties of the compounds such as their structures are not well known. This may be attributed in part to the complexity of the phase diagram and difficulty in obtaining single-crystal samples.

The title compound belongs to this series. It contains metal atoms with different valences as represented by the formula $Tl^{1+}(Tl^{3+}S_2^{2-})$. The first structural study of TlS was reported by Hahn and Klinger [3]. Utilizing powder x-ray diffraction data they concluded that TlS is isostructural to TlSe and has a tetragonal chain structure. However, recent single-crystal x-ray studies by the present authors [4, 5] revealed that TlS also crystallizes in a monoclinic structure.

Monoclinic TlS has a layer structure similar to the ternary compounds, such as $TlGaSe_2$ and $TlInS_2$ [6, 7]. These ternary thallium compounds were studied extensively by Russian researchers [8–10]. It was revealed that $TlGaSe_2$ and $TlInS_2$ undergo successive phase transitions accompanied by the soft ferroelectric mode. The structure of the intermediate phase is reported as incommensurate [11]. Details of the incommensurate and low-temperature phases, however, have not yet been reported.

In a recent paper, the present authors studied the phase transitions of monoclinic TlS by means of x-ray diffraction, dielectric and calorimetric measurements [4]. It was found that monoclinic TlS is ferroelectric at room temperature and upon heating it undergoes successive phase transitions at 318.6 K and 341.1 K. The phase above 341.1 K is paraelectric. The transition at 341.1 K is second order, while the lower one at 318.6 K is first order, having a temperature hysteresis of 1 K. Precession photographs taken at room temperature showed

0953-8984/93/254243+08$07.50

satellite reflections at $\frac{1}{4}$ along the c^* axis. These satellite reflections were found to disappear above 341.1 K.

The present x-ray measurements were performed to clarify the nature of the successive phase transitions in monoclinic TlS. The experiments show that the intermediate phase between 318.6 and 341.1 K is incommensurate. The phase sequence of TlS is similar to those of $TlGaSe_2$ and $TlInS_2$. A Landau-type phenomenological theory is applied to explain the successive phase transitions in TlS. The temperature behaviour of the dielectric constant is also discussed.

2. Experimental procedure and results

Single-crystal samples of monoclinic TlS were grown by direct reaction of the elements. Details of the sample preparation have been reported elsewhere [4]. The x-ray diffraction measurements were performed on a Huber four-circle diffractometer using graphite monochromated Cu Kα radiation. A cleaved sample was mounted on a goniometer head and set in a controlled air stream. The temperature was kept constant within 1 K by a PID controller. The unit cell parameters at 300 K are estimated as $a = 11.018$ Å, $b = 11.039$ Å, $c = 4 \times 15.039$ Å and $\beta = 100.69°$. The diffraction data were collected step by step in the reciprocal space at points on a grid with spacing 0.02 along both the a^* and b^* axes and 0.004 along the c^* axis.

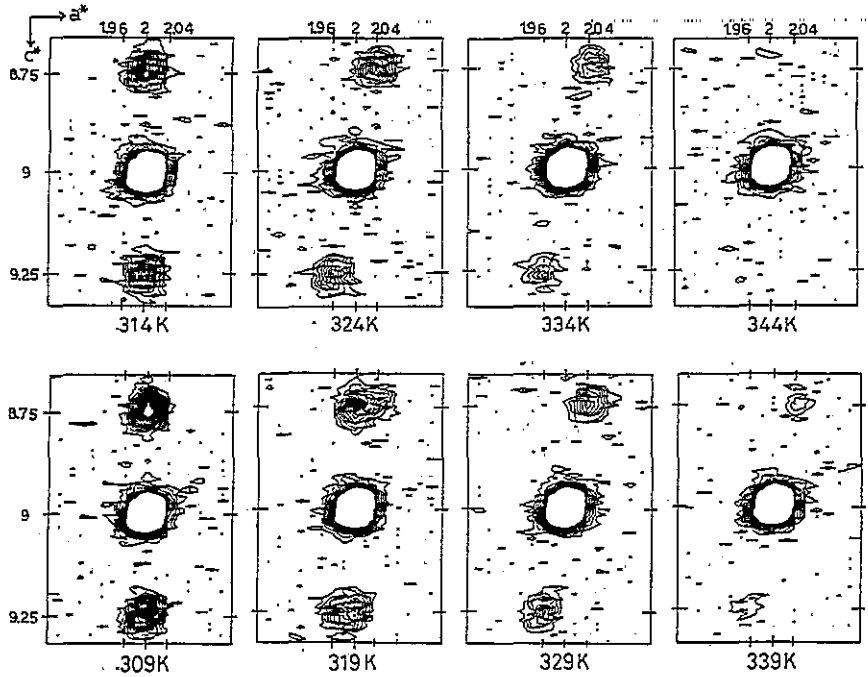

Figure 1. Temperature dependence of the contour patterns of the satellite peaks around the 229 main reflection. The lines are drawn at arbitrary units.

The temperature dependence of the contour maps of the satellite reflections is shown in figure 1. In the room temperature phase, satellite reflections are observed at commensurate

positions $q_c = (0, 0, \pm\frac{1}{4})$, suggesting fourfold modulations along the c axis. The intensities of the second-order satellite reflections (at $2q_c = (0, 0, \frac{1}{2})$) are very weak. Figure 2 shows the integrated intensities of the first-order satellite peaks plotted against the temperature. At the transition to the intermediate phase ($T_{IC} = 318.6$ K) the intensities of the satellite reflections decrease discontinuously and the peak position shifts from q_c to $q_i = (\delta', 0, \pm\frac{1}{4})$, where $\delta' = 0.04$. The contour pattern drawn in the vicinity of $T_{IC} = 318.6$ K shows the coexistence of the two peaks located at q_c and q_i, in agreement with the first-order nature of this transition.

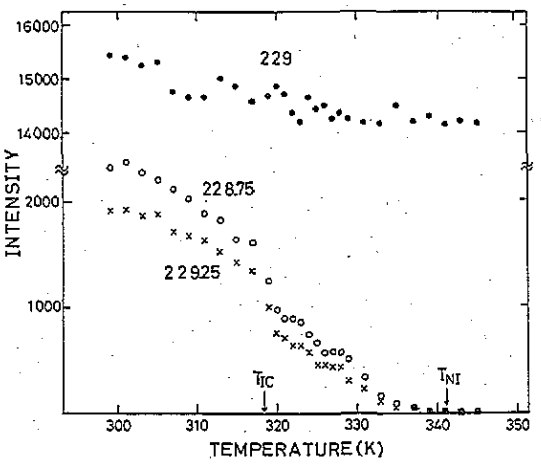

Figure 2. Temperature dependence of the integrated intensities of the main and satellite peaks.

Throughout the intermediate phase (318.6–341.1 K) the temperature variation of the modulation vector q is very little; in our experimental setting, the variation of the wave vector was not detected. As shown in figure 2, the intensities of the first-order satellites decrease with temperature. The intensities of the second-order satellites are quite weak; they were, in our measurements, under the count statistics. At the transition to the normal or paraelectric phase ($T_{NI} = 341.1$ K) these satellites disappear continuously, in agreement with the second-order nature of this transition. In the normal phase above 341.1 K, an attempt was made to detect the diffuse scattering at the position $q_i = (\delta', 0, \pm\frac{1}{4})$ but this did not succeed.

The dielectric constants of the sample were measured using an automatic bridge. The results have already been reported elsewhere [4] and are not reproduced here. The dielectric constant measured in the a–b plane shows a steep increase at T_{IC}, and a gradual divergence at T_{NI}, while the dielectric constant measured normal to the a–b plane shows little anomaly.

3. Analysis of the experimental results

Landau-type phenomenological approaches have succeeded in explaining the incommensurate phase transitions in several dielectrics [12, 13]. In a previous paper, Gashimzade *et al* [14] applied the theory to the incommensurate phase transition in $TlGaSe_2$. They discussed the temperature dependence of the dielectric constant applying the method given by Levstik *et al* [15]. Since at that time the available information on $TlGaSe_2$ was scarce,

their theory did not provide a correct description for the details of the phase transition. However, the essence of the phase transitions in the thallium chalcogen compounds is contained in their treatment, and we begin to describe the successive phase transitions in monoclinic TlS with a free energy expansion similar to theirs.

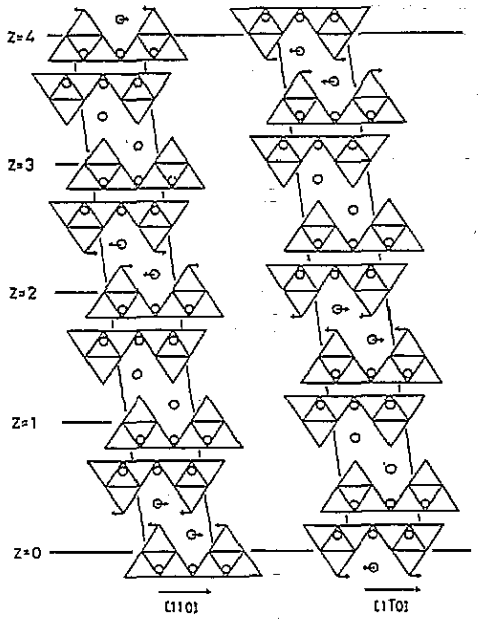

Figure 3. Schematic representation of the modulation observed in the room temperature phase (according to the single-crystal x-ray study [5]): projections along the [110] and [1$\bar{1}$0] axes. The triangles represent $Tl^{3+}S_4$ tetrahedra and the open circles represent Tl^{1+} ions. Arrows show relative displacements of the Tl^{1+} ions and the apical sulphur ions. Note that the displacements are expressed by a transverse optical mode with $q = (0, 0, \frac{1}{4})$, and that the local polarizations P_{110} and $P_{1\bar{1}0}$ alternate with a phase difference of about $\pi/4$. A detailed discussion of the modulation is given in [5].

The structure of the room temperature phase belongs to the space group $C2$ [5]. Figure 3 shows the displacement mode which characterizes the room temperature phase. The transition is ascribed to a condensation of a transverse optical mode with the wave vector q_c. The normal phase has the prototypic $TlGaSe_2$ structure [6, 7]. It belongs to the space group $C2/c$. The symmetry operations and irreducible representations corresponding to the point q_c are given in [14]. The relevant representation is two dimensional, and we introduce two compounds of the order parameter Q and Q^*, which transform as the bases of this representation. The free energy density is expanded in terms of the order parameter as

$$f(x) = (\alpha/2)QQ^* + (\beta/4)(QQ^*)^2 + i(\delta/2)(Q\,dQ^*/dx - Q^*\,dQ/dx) + (\kappa/2)(dQ/dx)dQ^*/dx + (\gamma/2)(Q^8 + Q^{*8}) + i\xi(Q^4 - Q^{*4})P + (\eta/2)QQ^*P^2 + P^2/2\chi_0 - PE \qquad (1)$$

where $\alpha = \alpha_0(T - T_0)$, β and $\kappa > 0$, and P is the polarization along the b axis. The third term is the Lifshitz gradient invariant, which leads to a spatially modulated phase. Here, the modulation is taken along the a axis, while it was taken along the c axis in [14]. The fifth term is the lock-in energy which stabilizes the commensurate phase. The sixth and seventh terms are the anisotropic and isotropic couplings between the order parameter and the polarization.

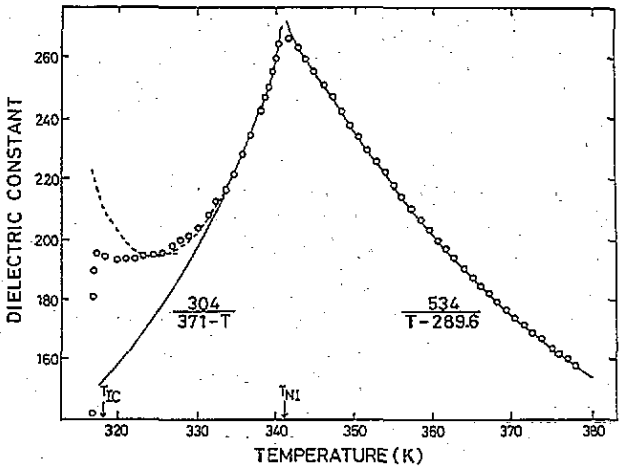

Figure 4. The temperature dependence of the observed and calculated values of the dielectric constant in the a–b plane of monoclinic TlS. The experimental values (open circles) were taken from [4]. The broken and full curves below T_{NI} represent calculated values with and without the anisotropic interaction between the polarization and the order parameter (see text).

The order parameter is transformed to polar coordinates ρ and ψ as $Q = \rho e^{i\psi}$ and $Q^* = \rho e^{-i\psi}$. From the minimization condition $\partial f/\partial P = 0$, P is written as

$$P = \bar{\chi}_0(E + 2\xi\rho^4 \sin 4\psi) \tag{2}$$

where $\bar{\chi}_0^{-1} = \chi_0^{-1} + \eta\rho^2$. Using the constant-amplitude approximation ($\rho(x) = \rho$) and substituting (2) into (1), we obtain

$$f(x) = (\alpha/2)\rho^2 + (\beta/4)\rho^4 + \delta\rho^2 \,\mathrm{d}\psi/\mathrm{d}x + (\kappa/2)\rho^2(\mathrm{d}\psi/\mathrm{d}x)^2 + \bar{\gamma}\rho^8 \cos 8\psi - \xi^2\rho^8\bar{\chi}_0 + 2\bar{\chi}_0\xi\rho^4 E \sin 4\psi - (\bar{\chi}_0/2)E^2 \tag{3}$$

where $\bar{\gamma} = \gamma + \xi^2\bar{\chi}_0$. Minimization of the free energy $\Phi = \int f(x)\,\mathrm{d}x / \int \mathrm{d}x$ with respect to ψ leads to the following Euler equation

$$\kappa\rho^2 \,\mathrm{d}^2\psi/\mathrm{d}x^2 + 8\bar{\gamma}\rho^8 \sin 8\psi + 8\bar{\chi}_0\xi\rho^4 E \cos 4\psi = 0. \tag{4}$$

The first integral of (4) becomes

$$\tfrac{1}{2}\kappa\rho^2(\mathrm{d}\psi/\mathrm{d}x)^2 = \epsilon + \bar{\gamma}\rho^8 - 2\bar{\gamma}\rho^8 \sin^2 4\psi - 2\bar{\chi}_0\xi\rho^4 E \sin 4\psi \tag{5}$$

where ϵ is the integration constant.

First, we will discuss the intensity of satellite reflections in the incommensurate phase. We will drop the lock-in and anisotropic interaction terms in (3) assuming that ρ is small. Then from (5) $d\psi/dx$ becomes a constant, and ψ can be set as $\psi = (q - q_c)_x x$ (a plane wave solution). Therefore, (3) can be rewritten as

$$f(q) = \tfrac{1}{2}\{\alpha_0(T - T_0) + 2\delta(q - q_c)_x + \kappa(q - q_c)_x^2\}\rho^2 + (\beta/4)\rho^4 \tag{6}$$

where the terms related to the electric field are dropped. The minimum of $f(q)$ occurs at $q_i = q_c + \delta/\kappa(1, 0, 0)$: the Lifshitz invariant term shifts the wave vector from the high symmetric point $q_c = (0, 0, \frac{1}{4})$ to $q_i = (\delta', 0, \frac{1}{4})$. The normal–incommensurate phase transition occurs at $T_{NI} = T_0 + \delta^2/\alpha_0\kappa$. The order parameter ρ varies with temperature as

$$\rho = [(\alpha_0/\beta)(T_{NI} - T)]^{1/2} \qquad \text{for } T < T_{NI}. \tag{7}$$

The observed linear temperature dependence of the satellite intensities I below T_{NI} can qualitatively be explained by (7), since $I \propto \rho^2$ (cf figure 2). In order to compare with theory, however, more precise intensity measurements are necessary.

Next, we will discuss the temperature dependence of the dielectric constant in somewhat more detail. If the anisotropic coupling term between the polarization and the order parameter is dropped, $x^{-1} = x_0^{-1} + \eta\rho^2$. The observed dielectric constant shows a Curie–Weiss type divergence in the normal phase where $\rho = 0$; see figure 4. In order to fit the experimental curve, we assume that

$$x_0^{-1} = (T - T_p)/C \tag{8}$$

where $T_p = 289.6$ K is the paraelectric Curie point and C is of the order of 500 K (see the full curve above T_{NI} in figure 4). This is in contrast to [14], where χ_0 was set to a constant assuming that there was no dielectric anomaly at the NI transition as usual for improper ferroelectrics.

The inverse dielectric constant in the incommensurate phase is expressed as

$$\bar{x}^{-1} = x_0^{-1} + \eta(\alpha_0/\beta)(T_i - T) \simeq (1/C')(T_{p'} - T) \tag{9}$$

where C' is of the order of 300 K and $T_{p'}$ is 371 K. The experimental values below T_{NI} are well fitted by (9) (see the full curve below T_{NI} in figure 4).

As the temperature is decreased further, however, the experimental values deviate from this curve. The deviation can be attributed to the omission of the anisotropic interaction term between the order parameter and the polarization. Then, (5) should be solved explicitly. Here we follow the technique developed by Sannikov [16, 17], using the elliptic function. The solution gives a regular soliton lattice. The net polarization is obtained by averaging over the period of the soliton lattice. The resultant dielectric constant is expressed as

$$\chi = \bar{\chi}_0 + (\chi_0^2\xi^2/\bar{\gamma})[E(k)/(1 - k^2)K(k) - 1] \tag{10}$$

where $k^2 = 2\bar{\gamma}\rho^8/(\epsilon + \bar{\gamma}\rho^8)$ and $K(k)$ and $E(k)$ are the complete elliptic integrals of the first and second kind, respectively [14]. The parameter k is determined by the condition $\partial\Phi/\partial k = 0$, i.e.

$$\rho^3 = \pi\delta(1/k\bar{\gamma})^{1/2}k/E(k). \tag{11}$$

The temperature dependence of the dielectric constant is estimated numerically using equations (7), and (9)–(11). The calculated curve qualitatively reproduces the experimental results (the broken curve in figure 4). As the incommensurate–commensurate (IC) transition is approached, the variation of the phase with respect to the electric field, $\partial\psi/\partial E$, tends to diverge. The divergence is, however, blocked by the first-order nature of the IC transition. The impurities included in the sample will also suppress the divergence by pinning the phase ψ. As described before, it was found that the wave vector is constant over the temperature range of the incommensurate phase. In the present case, therefore, there may be some other mechanism which not only suppresses the dielectric divergence but also stabilizes the commensurate structure having a period of $25 = 1/\delta'$ along the a axis.

Finally, we will discuss the relation between χ_0 and α. In the present paper, we assumed that $\chi_0 = C/(T - T_p)$, $\alpha = \alpha_0(T - T_0)$ and $T_0 > T_p$. As is seen in figure 4, for the order parameters Q and Q^* we can take the polarizations $P_{110}(q)$ and $P_{1\bar{1}0}(q)$, which alter with a phase difference of about $\pi/4$. In this sense α will correspond to $\chi(q)$, while $\chi_0 = \chi(0)$ since P is the uniform polarization along the b axis which is composed of P_{110} and $P_{1\bar{1}0}$. The interaction between the polarizations determines which structure appears in the ordered phase. The Fourier transform of the interaction is given by $\chi(q)$. The experimental results suggest that $\chi(q_c)$ is always lower in energy than $\chi(0)$. Although both modes have a tendency to become soft as the temperature is decreased, the modulation wave takes place along the c axis before the uniform polarization mode condenses. P is still produced through the anisotropic coupling, as (2) shows, when $\bar{\gamma} < 0$ and $8\psi = (2n + 1)\pi$.

In the thallium chalcogen series, $TlGaSe_2$ is the most popular, and many data have been accumulated as to its physical properties and the phase transitions. In a recent paper, Hochheimer *et al* [18] have investigated the phase transitions of $TlGaSe_2$ using dielectric, calorimetric, infrared and x-ray diffraction techniques. They reported that $TlGaSe_2$ undergoes successive phase transitions at 120 K and 110 K. The reported behaviour of the dielectric constant is very similar to that of TlS, although the temperature range of the intermediate phase is narrower. McMorrow *et al* [11] also studied the phase transitions of $TlGaSe_2$ by the triple-crystal x-ray diffraction technique. They reported that below 110 K the satellites appear at $q = (0, 0, \frac{1}{4})$, the same position as in TlS. In the intermediate phase between 110 K and 117 K, however, they reported that the satellites appear at $q = (\delta', \delta', \frac{1}{4})$ with $\delta' = 0.02$, instead of $q = (\delta', 0, \frac{1}{4})$. The origin of the difference between TlS and $TlGaSe_2$ should be clarified.

Acknowledgment

This work is supported in part by grants-in-aid for scientific research on priority areas from the Ministry of Education, Science and Culture, Japan.

References

[1] Asai C 1935 *Sci. Pap. Inst. Phys. Chem. Res.* **14** 797 (in Japanese)
[2] Nagat A T 1989 *J. Phys.: Condens. Matter* **1** 7921
[3] Hahn H and Klinger W 1949 *Z. Anorg. (Allg.) Chem.* **260** 110
[4] Kashida S, Nakamura K and Katayama S 1992 *Solid State Commun.* **82** 127–30
[5] Nakamura K and Kashida S *J. Phys. Soc. Japan* submitted
[6] Müller D and Hahn H 1978 *Z. Anorg. (Allg.) Chem.* **438** 258
[7] Henkel W, Hochheimer H D, Carlone C, Werner A, Ves S and v Schnering H G 1982 *Phys. Rev.* B **26** 3211

[8] Volkov A A, Goncharov Yu G, Kozlov G V, Allakhverdiev K R and Sardarly R M 1983 *Sov. Phys.–Solid State* **25** 2061
[9] Aliev R A, Allakhverdiev K R, Baranov A I, Ivanov N R and Sardarly R M 1984 *Sov. Phys.–Solid State* **26** 775
[10] Banis Yu, Brillingas A, Grigas I and Guseinov G 1987 *Sov. Phys.–Solid State* **29** 1906
[11] McMorrow D F, Cowley R A, Hatton P D and Banys J 1990 *J. Phys.: Condens. Matter* **2** 3699
[12] Levanyuk A P and Sannikov D G 1976 *Sov. Phys.–Solid State* **18** 245
[13] Ishibashi Y and Dvora'k V 1978 *J. Phys. Soc. Japan* **44** 32
[14] Gashimzade F M, Gadzhiev B R, Allakhverdiev K R, Sardarly R M and Shteinshraiber V Ya 1985 *Sov. Phys.–Solid State* **27** 2286
[15] Levstik A, Prelovsek P, Filipic C and Zeks B 1982 *Phys. Rev.* B **25** 3416
[16] Sannikov D G 1980 *J. Phys. Soc. Japan Suppl.* **49**B 75
[17] Sannikov D G 1986 *Incommensurate Phases in Dielectrics 1. Fundamentals* ed R Blinc and A P Levanyuk (Amsterdam: North-Holland)
[18] Hochheimer H G, Gmelin E, Bauhofer W, v Schnering-Schwartz Ch, v Schnering H G, Ihringer J and Appel W 1988 *Z. Phys.* B **73** 257